Magnetic moments of transition metals overlayers on fcc Ni surface

1998 J. Phys.: Condens. Matter 10 8679

(http://iopscience.iop.org/0953-8984/10/39/007)

J. Phys.: Condens. Matter **10** (1998) 8679–8686. Printed in the UK PII: S0953-8984(98)92584-X

Magnetic moments of transition metals overlayers on fcc Ni surface

Željko V Šljivančanin and Filip R Vukajlović
Institute of Nuclear Sciences 'Vinča', PO Box 522, 11001 Belgrade, Yugoslavia

Received 17 March 1998, in final form 19 June 1998

Abstract. We calculate the magnetization profile in the (111) surface of face-centred cubic (fcc) Ni covered by a monolayer or a bilayer of 3d and 4d transition metals. The observed trends can be explained as in earlier works in terms of the hybridization between d states of the overlayer element and Ni substrate, although some interesting specific behaviour of the magnetization in the surface of fcc (111) Ni covered with different d metals has been observed.

1. Introduction

In the past few years interface magnetism has developed into one of the most active areas of solid-state physics. The central issue in this field is the coupling of different magnetic materials across a common interface. Magnetic properties at such interfaces are intimately related to the phenomena of interlayer exchange coupling. Presently, the structural and magnetic properties of interfaces, prepared mostly by the deposition of ultra-thin magnetic films on various magnetic substrates, are the matter of intensive experimental investigations [1–5]. Semi-infinite metallic crystals and interfaces are systems with reduced translational symmetry. All theoretical attempts to describe these systems must take into account the loss of translational symmetry in the direction normal to the investigated surface or interface. One of the possible approaches to treat systems with two-dimensional (2D) translational symmetry is the standard one-electron band structure calculation applied to the systems with, so called, super-cell or slab geometry [6–8]. In order to exclude the influence of neighbouring interfaces on the results of investigations of the selected interface, it is necessary to choose a super-cell with too many atoms. This method is simple, but computationally very time consuming. A more natural way to treat surfaces and interfaces is to use the advantages of the Green function technique [9].

Recently, a new and efficient self-consistent Green function technique for structures with only 2D periodicity, based on the generalized tight-binding (TB) linear-muffin-tin-orbitals (LMTO) method was established by Skriver and Rosengaard [10]. This technique was improved further, by the same authors, on the basis of linear-response theory and a linearized version of the Dyson equation to improve the convergency [11]. That procedure cut the number of iterations by an order of magnitude, and gave results for the work function of 4d metals in excellent agreement with the full-potential LMTO slab method of Methfessel *et al* [8]. Furthermore, in the bulk calculations they have applied a second-order LMTO Hamiltonian, also used in the Green function technique, and obtained the kinetic energy by integration of the Green function on a complex energy contour. As a result an effective partial cancellation of errors and improved accuracy was obtained in the calculated work

0953-8984/98/398679+08$19.50

functions and surface energies. The most important aspect of the developed technique is the ability, within the atomic sphere approximation (ASA) and in TB representation, to generate the Green's function matrices for a real, 2D interface by a simple and efficient procedure.

On the other hand, new techniques for measuring magnetic properties of well defined surfaces, interfaces, and thin films were developed. These facts made it possible to tackle the problem of particular practical and theoretical interest: the modification of the magnetic moments which takes place when an Fe surface is covered by a few layers of 3d transition metals (for more details and experimental references see Mirbt *et al* [12]). The authors of [12] presented the results of the magnetization profile in the (100) surface of bcc Fe covered by a monolayer or a bilayer of 3d transition metal, which were in good agreement both with experiments and earlier calculations where they exist.

In this work, the results of the systematic theoretical study of the magnetic properties of face-centred cubic (fcc) (111) surface of another ferromagnetic metal Ni covered with a monolayer or bilayer of 3d and 4d transition metals are presented. We have calculated the magnetic moment through the interface region including that of the topmost Ni layer. In our calculations the size of the magnetic moment and total energies for monolayer and bilayer coverage of fcc (111) Ni surface have been considered.

We have calculated the magnetic moment profile and the total energy of the semi-infinite Ni system coated with one or two layers of transition metals. In the monolayer (bilayer) calculations the surface (the surface and subsurface) of the mono (double) d atom overlayer(s) has (have) been allowed to attain an arbitrary magnetic coupling to the Ni substrate.

To the best of our knowledge, there do not exist experimental results of magnetic measurements of Ni metal surface coated with 3d and 4d metals, so that the presented theoretical results are, in fact, predictions of a new behaviour of magnetic Ni covered with a thin film of different d metals.

2. Details of calculations

The TB LMTO Green function technique developed by Skriver and Rosengaard [10, 11], is based on the works of Andersen and collaborators [13–16]. This formalism employs the connection existing between the LMTO ASA Hamiltonian Green function in the orthogonal representation and the TB KKR (Korringa–Kohn–Rostoker) ASA Green function. The most convenient way to solve the eigenvalue problem is to work in the orthogonal representation, while the best way to treat the perturbation influenced by the existing interface is by TB representation. The Green function matrix of the LMTO ASA Hamiltonian is defined by the following equation

$$[z\hat{I} - \hat{H}^{\gamma}]G^{\gamma}(z) = \hat{I} \tag{1}$$

where z is a complex energy, H^{γ} is the LMTO Hamiltonian

$$\hat{H}^{\gamma}(\boldsymbol{k}) = C + \sqrt{\Delta}\hat{S}^{\gamma}(\boldsymbol{k})\sqrt{\Delta} \tag{2}$$

for the given $\boldsymbol{k}$-vector from the reciprocal space, and $\hat{I}$ is the unit matrix. Zone centre C, its width Δ, and parameter γ are obtained on the basis of self-consistent band structure calculations for an infinite crystal [16]. These parameters carry the information about individual atomic species which comprise the investigated crystal. The information about the crystal structure is contained in the structure constant matrix $S^{\gamma}(\boldsymbol{k})$. Potential parameters are combined to form the matrix of the potential functions, which plays the central role in

the TB LMTO formalism. The KKR ASA Green function matrix in the tight-binding representation is defined by the equation

$$[P^{\beta}(z) - S^{\beta}(\boldsymbol{k})]g^{\beta}(\boldsymbol{k}, z) = 1. \tag{3}$$

The elements of the diagonal potential matrix $P^{\beta}(z)$ satisfy the following scaling relation

$$[P^{\beta}(z)]^{-1} + \beta = [P^{\gamma}(z)]^{-1} + \gamma \tag{4}$$

where the diagonal screening matrix β is given in [16]. Within the orthogonal representation the potential function has a particularly simple form

$$P^{\gamma}(z) = \frac{z - C}{\Delta}. \tag{5}$$

Matrix elements of TB structure constants S^{β} have very short range in the real space and they can be easily calculated. The KKR ASA Green's function can be expressed through the LMTO ASA Hamiltonian Green's function

$$g^{\beta}(\boldsymbol{k}_{\parallel}, z) = -\frac{z - V^{\beta}}{\Gamma^{\beta}} + \frac{z - V^{\beta}}{\sqrt{\Gamma^{\beta}}} G^{\gamma}(\boldsymbol{k}_{\parallel}, z) \frac{z - V^{\beta}}{\sqrt{\Gamma^{\beta}}} \tag{6}$$

where

$$V^{\beta} = C - \frac{\Delta}{\gamma - \beta} \qquad \Gamma^{\beta} = \frac{\Delta}{(\gamma - \beta)^2} \tag{7}$$

and $\boldsymbol{k}_{\parallel}$ is a vector from the 2D Brillouin zone. The starting point in these calculations is the self-consistent one electron potential of an ideal 3D crystal, obtained from the standard band structure calculation results. Keeping the bulk values for the potential parameters and cancelling the interatomic interactions across the interface plane one can construct, a so-called, ideal Green function for the left- and right-hand side of the interface. The next step is to build, on the basis of these ideal left and right Green functions, the non-self-consistent interface Green function, by re-establishing the interatomic interactions across the interface plane. The existing interface leads to charge redistribution, as compared to the bulk electronic distribution of the constituents. The potential relaxation close to the interface for real systems, caused by this charge redistribution, may be taken into account by means of the following Dyson equation

$$g^{i} = g + g\Delta P^{i} g^{i}. \tag{8}$$

Transformation to the TB representation and use of a short-range basis set provide that the potential function relaxation $\Delta P = P^{i} - P$ is restricted to several layers on the both sides of the interface. Due to this, the interface Green function is obtained on the basis of solving a matrix equation of modest dimensions. On the other hand, the Hamiltonian Green function is directly connected with partial wave projected state density, while the moments of the state density are given by

$$m^{q}_{RL} = \frac{1}{2\pi \mathrm{i}} \oint \mathrm{d}z\, z^{q} \int_{SBZ} \mathrm{d}\boldsymbol{k}_{\parallel} G^{\gamma}_{RL,RL}(k_{\parallel}, z). \tag{9}$$

The energy contour integration in the lower half-plane should enclose all occupied states and cut the real axis at the Fermi level E_F, while the $\boldsymbol{k}_{\parallel}$-integration is performed over the 2D surface Brillouin zone (SBZ). In the self-consistent calculations only the first several moments of the state density with $q = 0, 1, 2$ are necessary. These moments contain all the information obtained from the electronic structure needed for the electron density calculations. The self-consistency procedure comprises the determination of electron density on the basis of the Hamiltonian Green function, the one-electron potential calculation, and

Dirac's equation solution. Using the obtained potential parameters, a new potential function is assembled, and Dyson's equation for the KKR-ASA Green function is solved. The KKR-ASA Green function matrix may be transformed into Hamiltonian Green's function matrix. The self-consistency procedure is terminated when the electrostatic dipole potential difference, in two successive iterations, drops below a fixed value defined by the accuracy required.

3. Results

Our calculations were based on the very natural approach to the interface problem based on a Green function technique [10, 11]. The applied technique serves as an extremely convenient way of obtaining a Green function for a real interface. The most important quality of this local-spin-density-approximation (LSDA) method is the ability, within the atomic-sphere approximation and in the tight-binding representation to generate the Green function matrices for a real 2D interface. This procedure is very simple, efficient, and it stays entirely within the ASA as far as the potential is concerned. However, for the charge density the dipole moments have to be included. If the accuracy of such an approximation is inadequate, i.e., the non-spherical terms to the atomic sphere potential are important, one may transform to a Hamiltonian Green function representation and proceed as in a conventional Green function calculation.

We have used the exchange-correlation functional of Vosko–Wilk–Nusair throughout the present work [17]. For k-space integration the 45 special points [18] have been used in the irreducible part of the 2D Brillouin zone. The bulk Ni Wigner–Seitz (WS) radius of 2.602 a.u. was chosen for all other elements, and lattice relaxation has been neglected. The LSDA bulk Ni calculations produce a ferromagnetic solution with spin magnetic moment of 0.64 μ_B per Ni site [19]. We have studied fcc (111) Ni surface, on which one or two layers of X (3d or 4d) element is added before reaching vacuum. For all calculations four Ni layers and three layers of empty spheres are allowed to differ from respective bulk values. The energy contour integration may be reduced to a semicircle in the lower half-plane and performed by means of a Gaussian integration technique with 16 points distributed exponentially on a semicircle in a complex plane, in order to emphasize the contributions close to the Fermi level [11]. The results for the self-consistent magnetic moment calculations for one and two added layers of 3d and 4d transition metals on the top of fcc (111) Ni surface layer are presented in figures 1 and 2. There exists the noticeable difference between these results and the earlier results obtained when bcc(100) Fe surface was covered by the same number of 3d transition metal layers [12]. The bcc iron is characterized by noticeable exchange splitting. The 3d band centres for electrons with 'up' and 'down' spin states are separated by 0.16 Ry. Because of that, the covering of Fe with one or two layers of early transition metals (ETM: Ti–Cr), whose 3d bands lie energetically higher than Fe 3d bands, caused the more pronounced hybridization with Fe spin 'down' 3d states. As a result, the bigger fraction of spin-down 3d states of ETM found in the energy region of Fe 3d states is increased, and since the Fermi level is situated in this region, antiferromagnetic coupling follows. For the late transition metals (LTM: Mn–Cu), the situation is reversed, and the coupling to substrate is ferromagnetic.

Exchange splitting between d 'up' and 'down' states for ferromagnetic Ni is very small, 0.05 Ry. One can not surmise such general conclusions about different degrees of hybridization among the substrate and non-magnetic overlayers only on the basis of the positions of their zone centres. In the case of an added layer of some of the ETM (Ti, V, Zr, Nb) the small induced magnetic moment with the same sign as the Ni magnetic moment

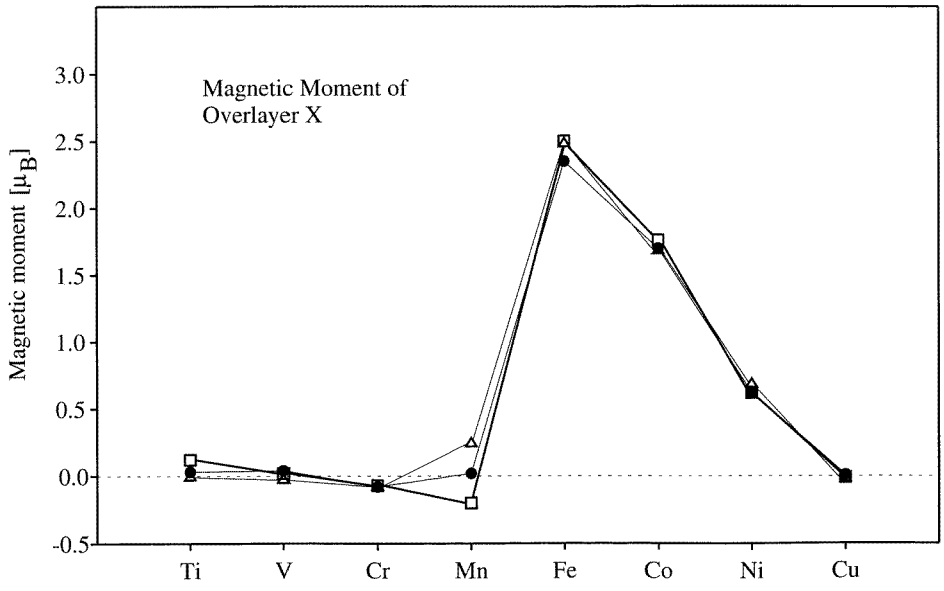

Figure 1. The magnetic moment for fcc (111) Ni surface coated by one and two layers of 3d transition metals X (X = Ti, . . . , Cu). The squares correspond to the magnetic moment of the surface layer for the case of the monolayer covered Ni surface. The triangles and circles correspond to the magnetic moment of 3d transition metal of the surface and the subsurface layer, respectively, for the case of bilayer covered Ni surface.

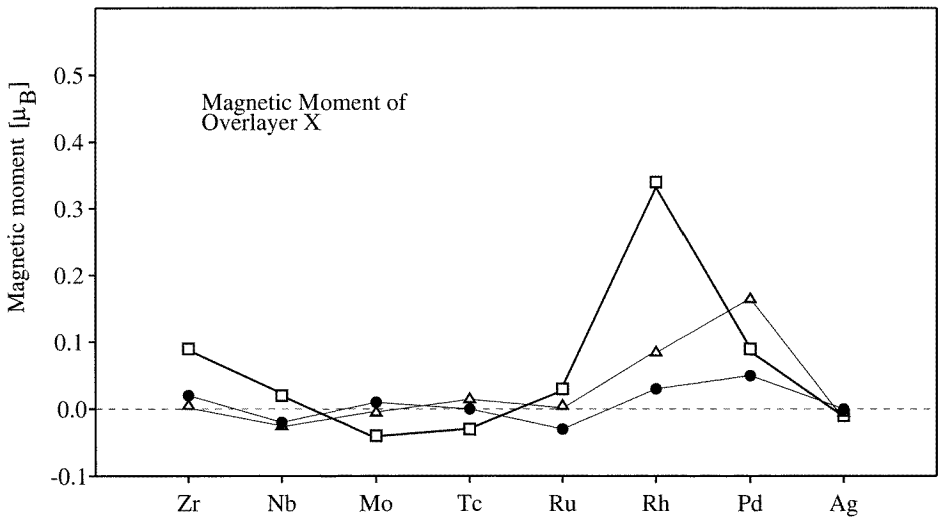

Figure 2. Same as in the figure 1, but for the Ni fcc (111) surface coverage with 4d transition metals X (X = Zr, . . . , Ag).

appears, while for Cr and Mo we obtain antiferromagnetic coupling and the magnetic moment of different signs on the overlayer atoms. We have the same results for the first atoms of the 3d and 4d LTM series (Mn and Tc). Generally speaking, the situation for LTM

is not quite clear and definite. Their d band centres are situated below the Ni d band centre. At first sight, one could expect the induced magnetic moment on the overlayer atoms to be the same sign as that of Ni. This is the case for Ru, Rh, and Pd, whose band centres are closer to the Ni band centre. In the case of Ag and Cu as the overlayer atoms on Ni substrate, very small magnetic moments of different signs are induced. Their d band centres are significantly lower than Ni 3d band centres, and the hybridization is very weak. When the absolute value of the induced magnetic moment is relatively small, then the details of the density of states curve for the overlayer elements are important in the determination of the induced magnetic moment sign.

If well known antiferromagnetic metals Cr and Mn are added in the form of one or two layers on the Ni fcc(111) surface, the size of the induced magnetic moments are significantly lower than if the body-centred cubic (bcc) Fe is used like a substrate material. Let us note here, that bulk band structure calculations of Cr and Mn with WS radius of 2.602 a.u. characteristic for fcc Ni, give paramagnetic solutions for these metals. This result can be easily comprehended if one looks at the surface atom arrangements. The chromium and manganese atoms, adsorbed on fcc (111) Ni surface, form 2D triangular lattice with the lattice parameter importantly lower than the respective triangular lattice parameters for pure surfaces of these antiferromagnetic metals. The smaller lattice parameter produces a bigger overlap of wavefunctions centred on different lattice sites. The well known band widening and magnetic moment lowering appears as a consequence of this lattice constant reduction. Calculated magnetic moments of Ni atoms in the atomic layer closest to the interface with 3d and 4d overlayers are shown in figure 3. As can be seen in figure 3 the Ni moment depends very delicately on the number of added transition metal layers and the atomic number of the coating material. In the case of coverage with ETM overlayer, the interface Ni magnetic moment is significantly lower than respective magnetic moments obtained in

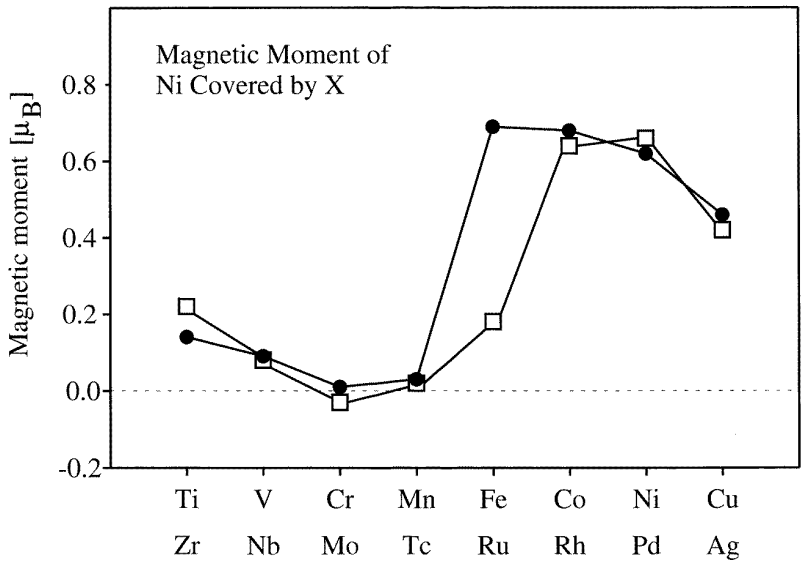

Figure 3. The calculated magnetic moment of Ni at the interface. The circles correspond to the calculated ground-state moment for the monolayer coverage with 3d transition metal X, while squares depict the calculated magnetic moment when the same Ni fcc (111) surface is covered by one layer of the 4d transition metal X.

bulk Ni calculations. The Fermi energy E_F cuts very narrow 3d spin 'down' bands, so that the density of these states at the Fermi energy is large. The pronounced peak in the 3d spin 'up' density of states is insignificantly below E_F. The interactions with 3d and 4d transition metal atoms of the coated materials bring about a lowering of the 3d-spin 'down' Ni band and a considerable reduction of the nickel atomic magnetic moment on the observed interface. Covering of fcc (111) Ni surface with one or two Fe, Co, Rh, or Pd layers does not produce essential changes in the values of magnetic moments of Ni atoms in the observed interface. This is the usual consequence of surface coordination number lowering for Fe and Co, as compared to the atomic coordination number in the respective bulk metal. The magnetic moments induced on the added layers of Rh and Pd atoms are 0.1 to 0.3 μ_B. It is well known that Rh and Pd are metals for which Stoner's criterion for the appearance of magnetic order

$$ID(E_F) > 1 \tag{10}$$

is almost fulfilled. In thin films of these metals this criterion can be fulfilled due to a probable increase of the state density at the Fermi level $D(E_F)$ (the Stoner parameter I usually keeps its atomic value).

4. Concluding remarks

In conclusion, it should be said that we have presented the results obtained for the surface profile of the magnetization of ferromagnetic Ni, when it is covered with a monolayer and bilayer of 3d and 4d transition metal atoms. In our calculations, for both monolayer and bilayer coverage of Ni fcc (111) surface with 3d and 4d transition metals, arbitrary magnetic coupling to Ni substrate has been allowed. We did not investigate any metastable solutions.

First, the magnetic coupling and the variation of magnetic moment across these transition metal series could be explained on the basis of similar grounds as in the earlier work of Mirbt *et al* [12], i.e. in terms of the hybridization effects between the Ni 3d states and the 3d and 4d states of covering metal, notwithstanding the fact that there exist some subtle differences in the behaviour of the interface magnetic moment of Ni coated with 3d transition metal atoms, as compared to the case of the interface magnetic moment of Fe coated with atoms from the same series. We have shown that these specific properties of Ni interface moments follow from the fact that the exchange splitting between majority and minority spin bands is very small in the case of Ni fcc transition metal.

The only fundamental discrete circuit elements that have been left behind in the revolution and rapid advances in solid-state electronics are those involving magnetic materials. In fact, in all of the advances made in electronic materials processing over the past two decades, very little work has been done to incorporate magnetic materials into planar integrated electronic (or photonic) circuitry (see, for instance, the work of Prinz [20]). The possibility of preparing ferromagnetic metals in thin-film form of definite layer thickness opens new possibilities for their applications. The most interesting outcome of our calculations of Ni coated with different transition metals, is the possibility to change the induced magnetic moment on the Ni interface and on the surface layers of added transition metals in the wide range of values. The value of the interface Ni magnetic moment in figure 3 ranges from $-0.03\ \mu_B$ (coating with Mo) to $0.69\ \mu_B$ (coating with Fe). This is a much wider relative range of changes than in the case of Fe covered with 3d transition metals (cf figure 2 in [12]). The range of values of magnetic moments induced on the layers of 3d and 4d metals, which cover the Ni fcc(111) surface, is similar to the respective range

obtained for Fe covered with 3d transition metals. These findings, if proved experimentally, could be of practical importance.

Acknowledgments

This work was supported by the Serbian Scientific Foundation under the project Physics of Condensed Matter and New Materials, grant No 3. We are very grateful to Dr H L Skriver for valuable advice and permission to use his new version of the computer code for the investigation of surfaces and interfaces. We also thank Z S Popović for stimulating discussions. This work has benefited scientifically from the European Community Human and Mobility programme Ψ_k network.

References

[1] Stearns M B, Lee C H and Groy T L 1989 *Phys. Rev.* B **40** 8256
[2] Purcel S T, Johnson M T, McGee N W E, Coehoo R and Hoving W 1992 *Phys. Rev.* B **45** 13 064
Walker T G and Hopster H 1993 *Phys. Rev.* B **48** 3563
[3] Vogel J, Panaccione G and Sacchi M 1994 *Phys. Rev.* B **50** 7157
[4] Wang Z Q, Lee Y S, Jona F and Marcus P M 1987 *Solid State Commun.* **61** 623
Pine P and Eymery J P 1994 *J. Magn. Magn. Mater*. **133** 493
[5] Engel B N, Weidmann M H, Van Leewen R A and Falco C M 1993 *J. Appl. Phys.* **73** 6192
[6] Fu C L, Freeman A J and Oguchi T 1985 *Phys. Rev. Lett.* **25** 2700
[7] Lee J I, Hong S C, Freeman A J and Fu C L 1993 *Phys. Rev.* B **47** 810
[8] Methfessel M, Hennig D and Scheffler M 1992 *Phys. Rev.* B **46** 4816
[9] Wiliams A R, Feibelman P J and Lang N D 1982 *Phys. Rev.* B **26** 5433
[10] Skriver H L and Rosengaard N M 1991 *Phys. Rev.* B **43** 9538
[11] Skriver H L and Rosengaard N M 1992 *Phys. Rev.* B **46** 7157
[12] Mirbt S, Erikson O, Johanson B and Skriver H L 1995 *Phys. Rev.* B **52** 15 070
[13] Andersen O K 1975 *Phys. Rev.* B **12** 3060
[14] Skriver H L 1984 *The LMTO Method* (Berlin: Springer)
[15] Andersen O K and Jepsen O 1984 *Phys. Rev. Lett.* **53** 2571
[16] Andersen O K, Pawlowska Z and Jepsen O 1986 *Phys. Rev.* B **34** 5253
[17] Vosko S H, Wilk L and Nusair M 1980 *Can. J. Phys.* **58** 1200
[18] Cunningham S L 1974 *Phys. Rev.* B **10** 4988
[19] Dreyssé H and Demangeat C 1997 *Surface Sci. Rep.* **28** 65
[20] Prinz G A 1990 *Science* **250** 1092